ADVANCED OPTICAL MATERIALS
www.advopticalmat.de

Mitigation of the Moiré Effect in Overlapped Optical Films by Lateral Buckling of Sharp Edges of Prism Arrays

Yonghyeon Lee, Seong Gil Heo, Min-Gi Jo, Chaerim Lee, Enkhmandakh Enkhtaivan, Hyemin Lee, and Hyunsik Yoon**

The moiré effect arises from the superposition of periodic structures with differences in periods or angles. Although the moiré effect can be exploited as an intriguing tool to fabricate complex metastructures, reduction of the moiré effect can be an important issue in display technology that uses many optical films with periodic patterns. Because of the superposition, dark and bright regions can be seen by the naked eye, which is a reason for the degradation of the visual quality. In this work, the lateral deformation of shape edges of prism films is harnessed to reduce the moiré effect. After the preparation of a microprism array with hydrogel materials, the hydrogel microprism array is swelled via penetration of water molecules into the hydrogel networks. Due to the compressive stress applied by volume expansion with confinement, only the sharp edges laterally buckle randomly. The swollen hydrogel prism array is replicated by photopolymerization, and prism arrays with laterally buckled edges are obtained. The randomized edges help reduce the moiré effect of the optical film when the prism array is overlapped with other periodic devices, such as other prism arrays or display devices consisting of microscale pixels, without a significant decrease in the optical performance.

1. Introduction

Moiré patterns can be seen when more than two periodic patterns are superposed.[1] The optical interference of periodic patterns results in alternating bright and dark fringes due to the multiplication of the reflection/transmittance of the overlapped gratings. The optical patterns from the moiré effect can be seen when the period of the patterns is larger than the wavelength of visible light. Recently, the moiré effect has received attention because the effect can be observed in the superlattice of nanomaterials.[2–6] In addition, the moiré effect can be used for measurement methods such as alignment in nanoimprint lithography[7–9] and to fabricate complex metasurfaces by using the interference of nanopatterns.[2,10] Although the usage of the moiré effect has been extended to various fields, it is undesirable in display devices such as liquid crystal displays (LCDs) or organic light-emitting diodes (OLEDs). In display panels, pixel-defined patterns such as the black matrix should be periodic, and the moiré effect is inevitable when we use optical films with periodic patterns such as metal grids for tough screens, prism films for enhancement of the brightness, and lenticular lenses for an autostereoscopic display.[11] To reduce the moiré effect, the concept of randomization could be exploited. However, fabricating randomized structures in large areas is difficult.[12]

Here, we proposed a method to mitigate the moiré effect by using randomly buckled sharp edges in microprism arrays. Buckling phenomena have been used to fabricate micro- and nanoscale structures.[13–22] Bilayer systems, which have two layers with different moduli, have been well studied to produce periodic buckled structures by minimizing the total energy, such as the bending energy of thin-deposited films and the deformation energy of substrates.[13–16] Their applications include optical devices, microfluidic systems, and stretchable electronics.[13–16] Another approach is the delamination of patterned thin films from substrates to realize 3D structures, that can be exploited for wearable devices.[17,18] Although buckling methods have been developed to fabricate various nano- and microshapes, few studies have been conducted on the application of the lateral buckling of sharp edges. Lateral buckling is the phenomenon observed when a compressive stress is applied to high-aspect-ratio patterns.[19–22] Several methods to apply compressive stress for the formation of lateral buckles have been reported. Examples include use of the residual compressive stress during metal deposition on one face of nanowalls,[19] compressive bending of elastomeric blocks with line arrays embedded on their surfaces,[20] and volume expansion of confined microline patterns by swelling of hydrogel structures.[21,22] In this study, we used the lateral buckling of sharp edges in microprism arrays to avoid moiré patterns. By using multiple replication steps, we prepared prism arrays with hydrogel materials. After swelling of the hydrogel in water, expanded volume and deformation of sharp edges can be observed.

Y. Lee, M.-G. Jo, C. Lee, E. Enkhtaivan, H. Lee, H. Yoon
Department of Chemical and Biomolecular Engineering
Seoul National University of Science and Technology
Seoul 01811, Republic of Korea
E-mail: hmlee0208@seoultech.ac.kr; hsyoon@seoultech.ac.kr
S. G. Heo, H. Yoon
Department of Energy and Chemical Engineering
Seoul National University of Science and Technology
Seoul 01811, Republic of Korea

The ORCID identification number(s) for the author(s) of this article can be found under https://doi.org/10.1002/adom.202300539

DOI: 10.1002/adom.202300539

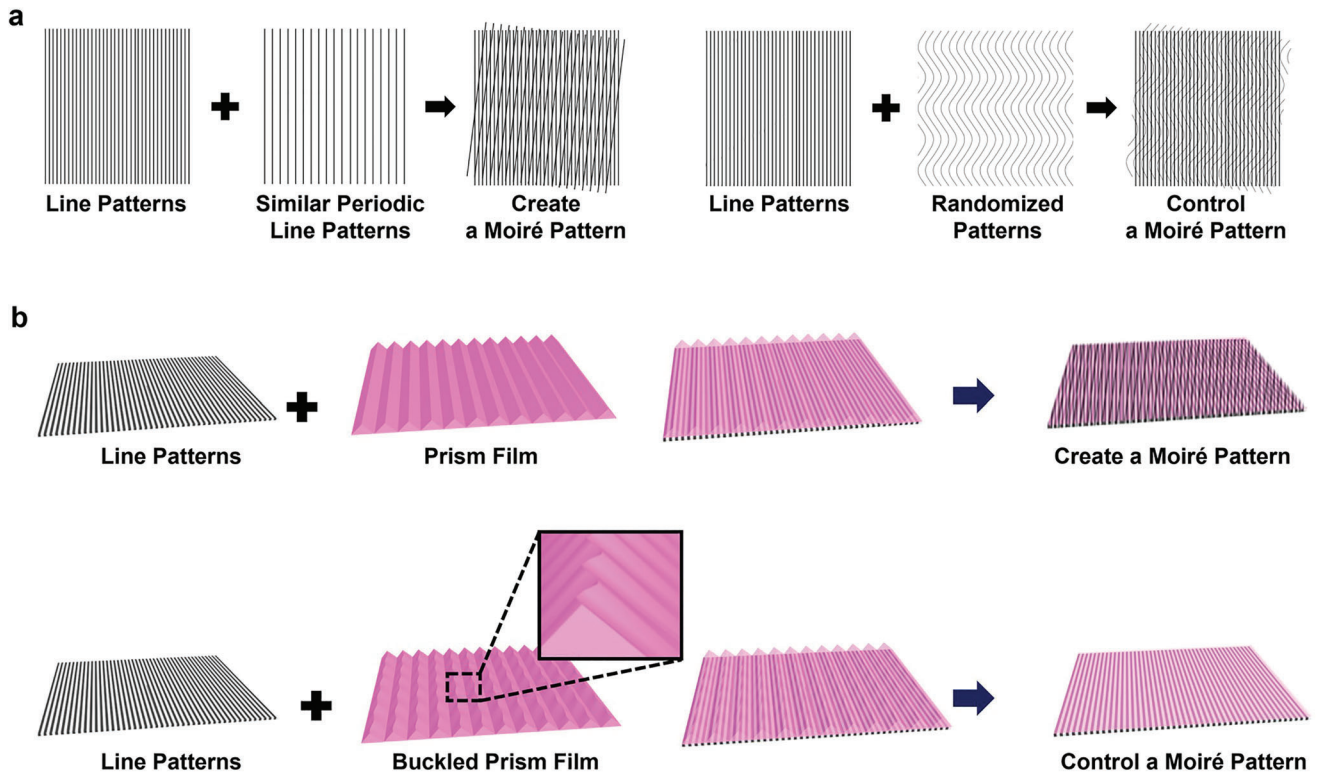

Figure 1. a) Schematic illustration explaining the moiré effect induced by overlapping periodic patterns and the concept of mitigating the moiré effect by randomizing patterns. b) Schematic illustration of the experiments. When we overlap the microprism array on a line pattern, the moiré effect can be seen. When we overlap microprism arrays with lateral buckling on the edges, the moiré effect can be reduced.

Under the condition of selective lateral buckling of sharp edges of prism films, we could reduce the moiré effect when we overlapped two optical films or superimposed films with randomized lateral buckles on a display device. We measured the transmittance at various viewing angles and controlled the viewing angle using prism arrays; thus, the moiré-mitigated films maintained the optical performance of the original prism arrays.

2. Concept of Mitigating the Moiré Effect via Laterally Buckled Edges of Prisms

Figure 1a shows a schematic illustration of the formation of a moiré pattern and the concept of the mitigation of a moiré pattern by overlapping randomized patterns. When two line patterns with similar periods are overlapped or slightly tilted, moiré patterns can be created due to the interference of two line patterns. When one of the line patterns is randomized, by contrast, the moiré patterns can be reduced, as shown in the conceptual picture of Figure 1a. Figure 1b shows a conceptual illustration of this work to mitigate moiré effects when overlapping a display device and a film with a microprism array on its surface. When we place a prism array film on a display device consisting of pixels such as an LCD or an OLED, we can see moiré patterns through the films. To mitigate this effect, we proposed a method to use randomized buckling of prism edges, which is formed by deformation of the prism edges under applied compressive stress. In this work, we exploited the volume expansion of hydrogel structures by swelling hydrogels through the absorption of water molecules within their internal networks. As shown at the bottom of Figure 1b, the randomized prism array showed a reduction in the moiré effect when we overlapped prism arrays with laterally buckled edges.

2.1. Fabrication of Prism Arrays with Laterally Buckled Edges

Figure 2a shows the experimental procedure of the fabrication of a prism array with laterally buckled edges and optical microscopy (OM) images and a scanning electron microscopy (SEM) image from the experimental results. First, we prepared a master pattern of prism arrays fabricated by micromachining methods. The detailed preparation method of the microprism array can be seen elsewhere.[23,24] In this experiment, we used a prism array with a period of 60 μm and a height of 30 μm (first column in Figure 2). After the fabrication of prism arrays, we replicated the pattern with polydimethylsiloxane (PDMS). We poured the mixture of the PDMS prepolymer and curing agent (mixing ratio = 10:1) on the master and detached it after curing for more than 4 h at 60 °C in an oven. Then, we replicated the inverted structures with hydrogel materials from PDMS molds. We prepared mixtures of photocurable hydrogels consisting of a photoinitiator (2-hydroxy-2-methyl-propiophenone), hydroxyethyl methacrylate (HEMA), acrylamide, and methacrylic acid. The swelling ratio can be controlled by the mixing ratio of the components (Figure S1,

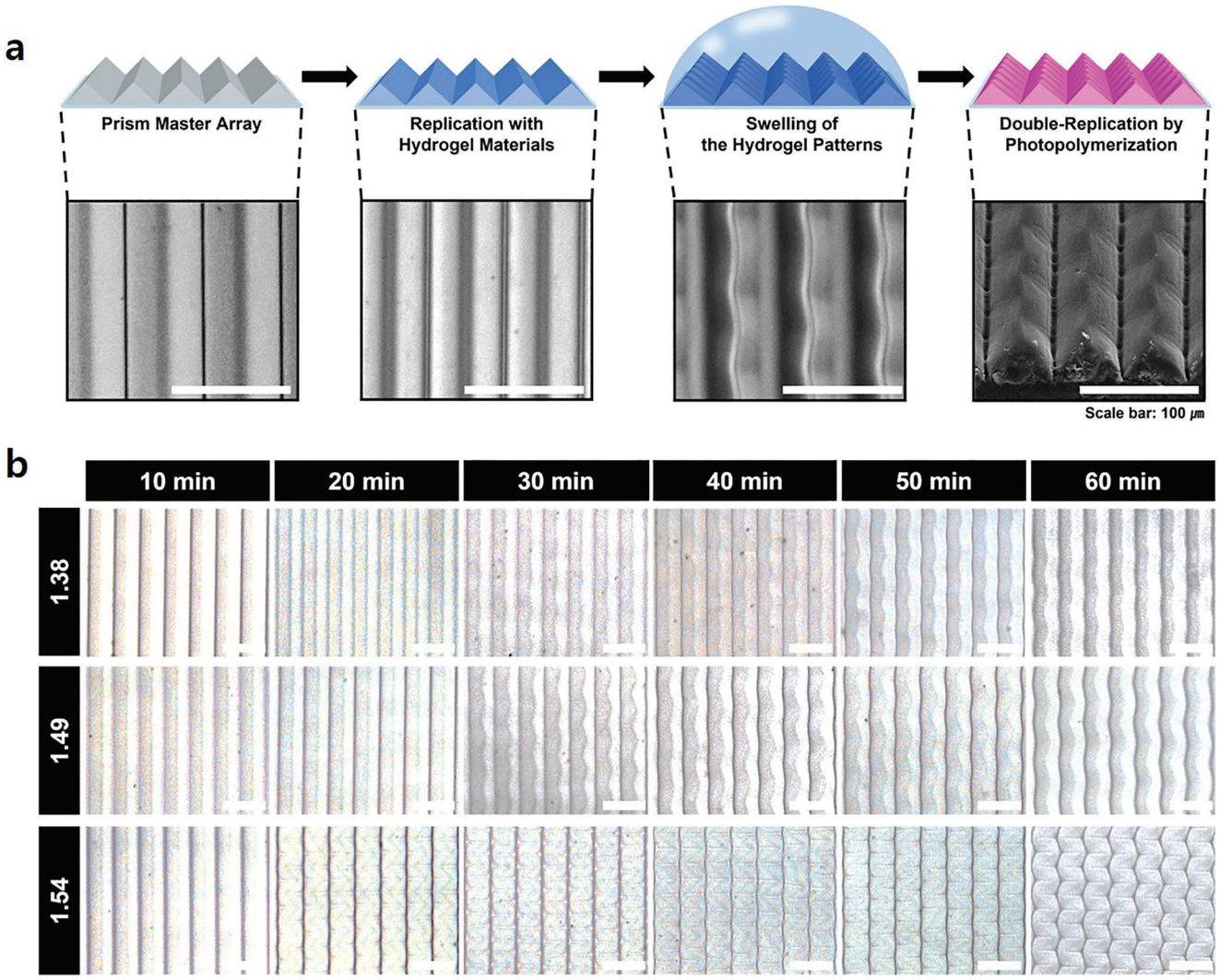

Figure 2. a) Schematic illustration of the fabrication of a microprism array with laterally buckled edges. After the preparation of a microprism array by hydrogel materials, the sharp edges of the prism were laterally buckled, and we fabricated a microprism array with buckled edges by double replication with other polymers. b) Images showing the changes in morphology over swelling time. Scale bars represent 100 μm.

Supporting Information). Then, we dropped the photocurable liquid on the PDMS mold and covered polyethylene terephthalate (PET) film on the prepolymer to prevent the diffusion of oxygen, which inhibited photopolymerization. To fill the liquid mixtures into the voids of the PDMS mold, we applied pressure and observed the removal of air between the liquid and the PDMS molds. Then, we performed UV light exposure (50 J s^{-1} m^{-2}) to crosslink the mixtures of monomers and detached the solidified prism array attached to PET films from the PDMS mold. The prism arrays with hydrogel materials can be seen in the second column of Figure 2a. The fabricated hydrogel patterns attached to the PET prism film were dipped in water for 1 h for swelling. During swelling, water molecules penetrated into the internal networks of the hydrogel patterns and induced volume expansion of the hydrogels.[21,22,25] Since the bottom of the hydrogel patterns was fixed to the PET substrate, when the hydrogel was swollen, only the top edges of the prism arrays were laterally buckled because of the compressive stress induced by the volume expansion in constrained conditions. The swollen hydrogel patterns can be observed by OM, as shown in the third column of Figure 2a. The upper part of the prism arrays was wrinkled, and the bottom was not severely deformed by swelling. To replicate the swollen hydrogel patterns, we filled a UV-curable hydrophobic perfluoropolyether (PFPE) prepolymer into the voids of the swollen hydrogels after removing water on the surface of the hydrogels. During UV crosslinking, the water molecules within the swollen hydrogels can be maintained because the water did not diffuse into the fluoro-prepolymer.[21] The detailed experimental procedure can be found in the Supporting Information (Figure S2, Supporting Information) and previous literature.[21] After double replication with polyurethane acrylate (PUA), we replicated the swollen shapes of hydrogel structures. The last column of Figure 2a shows an SEM image of PUA patterns replicated from PFPE. The tilted SEM image shows that the upper part of the prism arrays was deformed by compressive stress and that the bottom was fixed on the substrate.

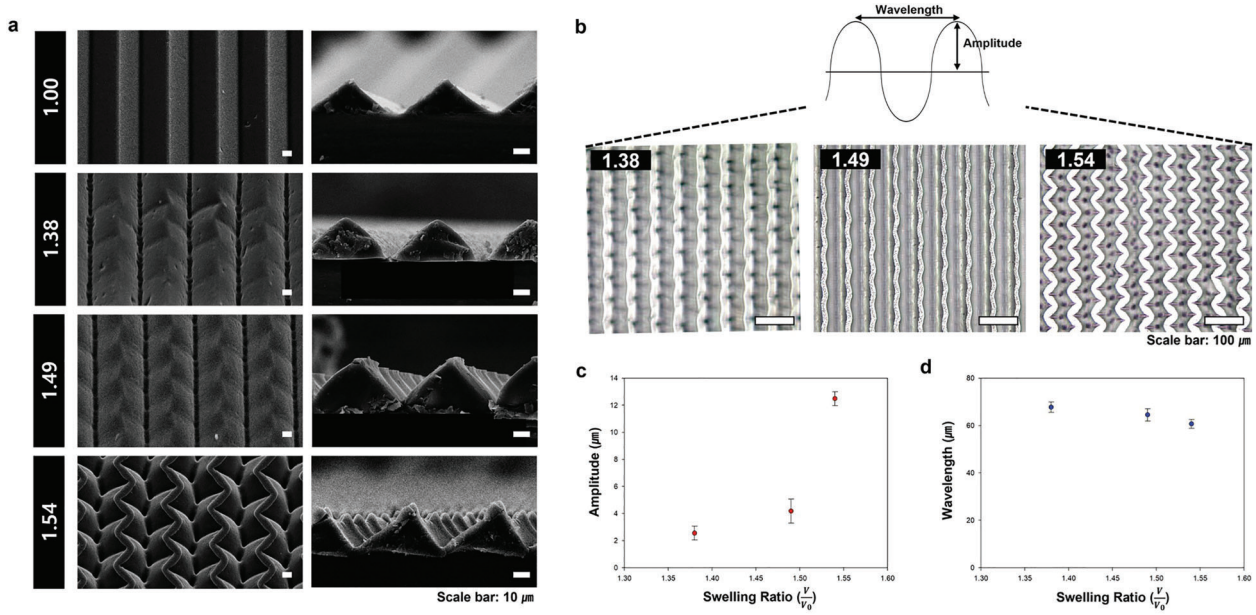

Figure 3. a) Tilted and cross-sectional SEM images of microprism arrays fabricated by replication of hydrogel shapes at different swelling ratios. b) Planar images obtained with an optical microscope of replicated samples with different swelling ratios. c) Graph showing the amplitude change with the swelling ratio. d) Graph showing the wavelength versus swelling ratio.

2.2. Control of Lateral Buckling of Prism Edges by the Swelling Ratio

To control the shape of the buckling in prism arrays, we adjusted the swelling ratio by changing the mixing ratio of methacrylic acid. Since methacrylic acid is hydrophilic due to its carboxylic acid groups, the swelling ratio was increased with higher amounts of methacrylic acid. When the samples were immersed in a water bath for 60 min, the measured swelling ratios ($\beta = (V/V_0)$, where V *is* the volume after swelling, and V_0 is the volume before swelling) were 1.38, 1.49, and 1.54. The methods used for measuring the swelling ratio have been described in the Experimental Section and in a previous study.[21] Figure 2b shows the changes in morphology over swelling time. When the swelling time was 10 min, the shape did not change. At swelling ratios of 1.38 and 1.49 (which were defined by the swelling ratios after 60 min), the edge areas began to buckle after 30 min. By contrast, at the swelling ratio of 1.54, the deformation developed from apexes to bottoms after 20 min of swelling. This phenomenon is similar to that observed in a previous study on the buckling of prism edges by applying compressive stress to elastomeric prisms.[26] In their study, the prism edges buckled when the prism angle was less than 90°. When the prism angle was >90°, localized creases initiated at the apexes and extended to the bottom.[26] In this study, we used a prism with an angle of 90°, which is the condition of a conventional brightness-enhancing film.[27] Two different deformation modes were observed: edge buckling at a low degree of swelling and crease development at a high degree of swelling. The mechanism is different from the previous study with elastomeric prisms[26] because the swollen hydrogel structures fixed on a substrate can be applied by compressive stress and the modulus became lower due to the interpenetration of water molecules inside the hydrogel networks. **Figure 3**a shows tilted (45°) and cross-sectional SEM images of prism arrays with different swelling ratios. Before swelling, the edge of the prism array was straight, as shown in the first row of Figure 3a. When the swelling ratio was increased, the deformation of prism shapes was greater due to the increased compressive stress. In particular, when the swelling ratio was 1.54, the bottom of the prism array could also be deformed. Under swelling ratios of 1.38 and 1.49, the valleys of the prism array were straight, and only the prism edges were buckled. The inverted shape of Figure 3a, which can be obtained by replica molding, can also be seen in Figure S3 of the Supporting Information. As shown in the cross-sectional SEM images, the overall prism angle was not significantly changed from that of the original prism array sample before swelling.

Figure 3b,c displays graphs showing the amplitude and wavelength of the wrinkles of prism arrays according to the swelling ratio. As the swelling ratio increased from 1.38 to 1.49, the amplitude slightly increased to 2.6 and 4.2 μm. Interestingly, the amplitude rapidly increased to 12.5 when the swelling ratio was 1.55. Based on the OM images in Figure 3b, the surface of the edges buckled until the swelling ratio was 1.49. However, the laterally buckled shapes became laterally folded shapes when the swelling ratio was 1.54, as shown in the third column of Figure 3b. The laterally folded shapes can also be seen in the fourth row of Figure 3a. This occurred because the confinement of the bottom was not maintained when the swelling ratio increased. The wavelengths slightly decreased to 67.742, 64.508, and 60.712 μm.

2.3. Mitigation of the Moiré Effect by Laterally Buckled Prism Films

Then, we conducted experiments to confirm the mitigation of the moiré effect with prism arrays with laterally buckled edges. **Figure 4**a shows the formation of moiré patterns observed by an

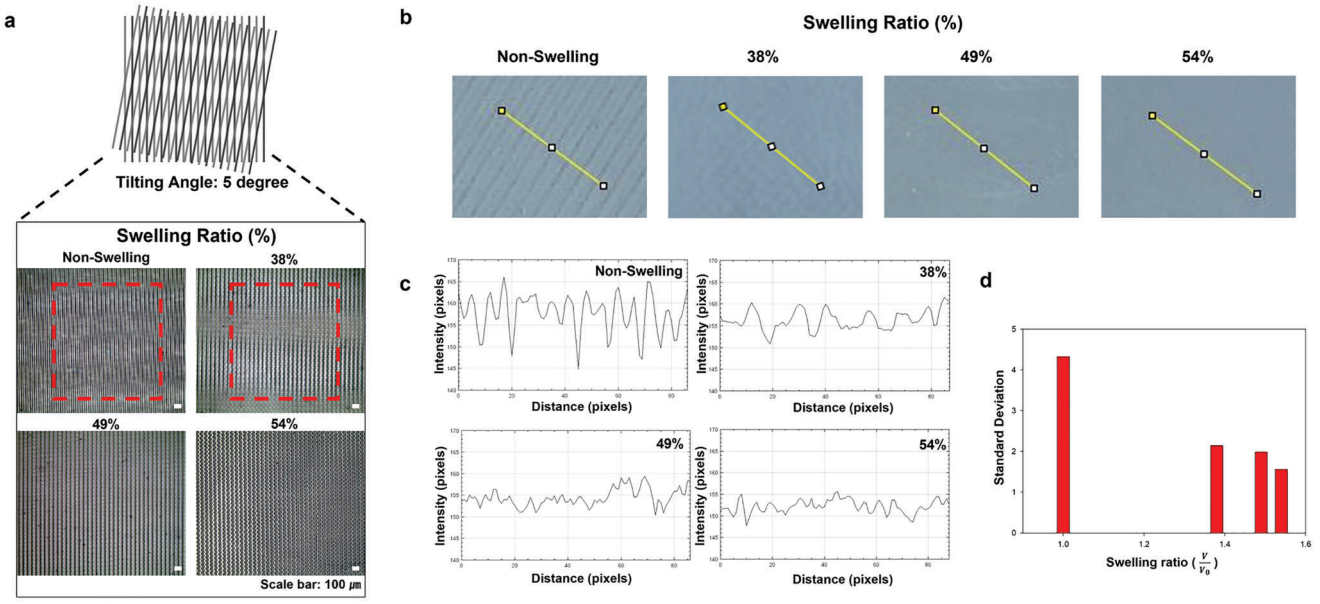

Figure 4. a) Moiré effects when overlapping the optical films fabricated under different conditions (swelling ratios) on an original prism array with a tilt angle (5°). b) Captured images of display devices after placing the optical films on the display panels. c) Graph showing the intensity distribution along the contours of (b). d) Standard deviation of the intensity of display devices through optical films fabricated by replication of hydrogel patterns swollen at different swelling ratios.

optical microscope when the buckled prism arrays were overlapped on the original prism arrays with a tilt angle of 5°. As shown in Figure 4a, moiré patterns can be found when the film is overlapped by prism arrays before swelling and after swelling with a swelling ratio of 1.38. Interestingly, moiré patterns were not found when we overlapped the prism arrays with laterally buckled shapes at the edges (swelling ratios of 1.49 and 1.54). To investigate the mitigation of the moiré effect, we took pictures of a screen of a display device (Galaxy J7 prime, Samsung) after placing the prism arrays on the screen. The specification of the display on which the film was placed is 401 ppi, which is 1 pixel per 63 μm when converted into micrometers (Figure S4, Supporting Information).

Figure 4b shows a photograph confirming the formation of moiré patterns with the eye when the buckled films with different swelling ratios were placed upright on the actual mobile phone display. As shown in Figure 4a, moiré patterns were found in the case of the nonswollen film and the film with a swelling ratio of 1.38. By contrast, moiré patterns were not found when we placed prism arrays with laterally buckled edges with swelling ratios of 1.49 and 1.54 on the display. To compare the degree of the moiré effect more quantitatively, the intensity was measured from the pictures in Figure 4b. Figure 4c shows graphs of the intensity scanned along the yellow lines of Figure 4b. If there were moiré patterns on the screen, then bright and dark parts could repeatedly appear in the image because of the moiré effect, and the difference in intensity could be large. By contrast, when there was no moiré effect on the screen, the intensity difference was small. Figure 4d shows a graph of the standard deviation of Figure 4c. When we placed the prism array without swelling on the display, the standard deviation was the highest, and the deviation decreased with increasing swelling ratio. The moiré patterns have periods that can be changed by varying the tilt angle between the two line patterns, as follows[11]

$$\lambda_{\text{moir'e}} = \lambda_{\text{prism}}/2\sin\left(\frac{\alpha}{2}\right) \quad (1)$$

where $\lambda_{\text{moiré}}$ is the period of the moiré patterns, λ_{prism} is the period of the prism arrays (= 60 μm in this study), and α is the angle between the two prism arrays. When we measured the moiré period with respect to the tilt angle, as shown in Figure S5 of the Supporting Information, the period was dependent on the tilt angle (α), and the experimental results were in good agreement with Equation (1). We highlight that the moiré effect was mitigated by the edge buckling of the prism arrays, regardless of the tilting angle. This is because the moiré pattern is generated by overlapping two straight line patterns, and the buckled patterns deviated from the straight lines in a random manner. When the deviation from the line axis is small (swelling ratio of 1.38), slight moiré patterns are observed. When the amplitude of buckling is increased, the deviation of the patterns from the line axis increases, and the moiré patterns disappear.

2.4. Optical Performance of Prism Arrays with Laterally Buckled Edges

For usage as an optical film, the prism array with deformed shapes should have similar performance to the original prism array. Because prism arrays are known for their collimation function,[27] we measured the luminance at different viewing angles. **Figure 5**a shows a graph of the luminance measurements at different viewing angles of prism arrays without and with deformation by swelling. Under swelling ratios of 1.38 and 1.49, the light was condensed similarly to with the original prism array.

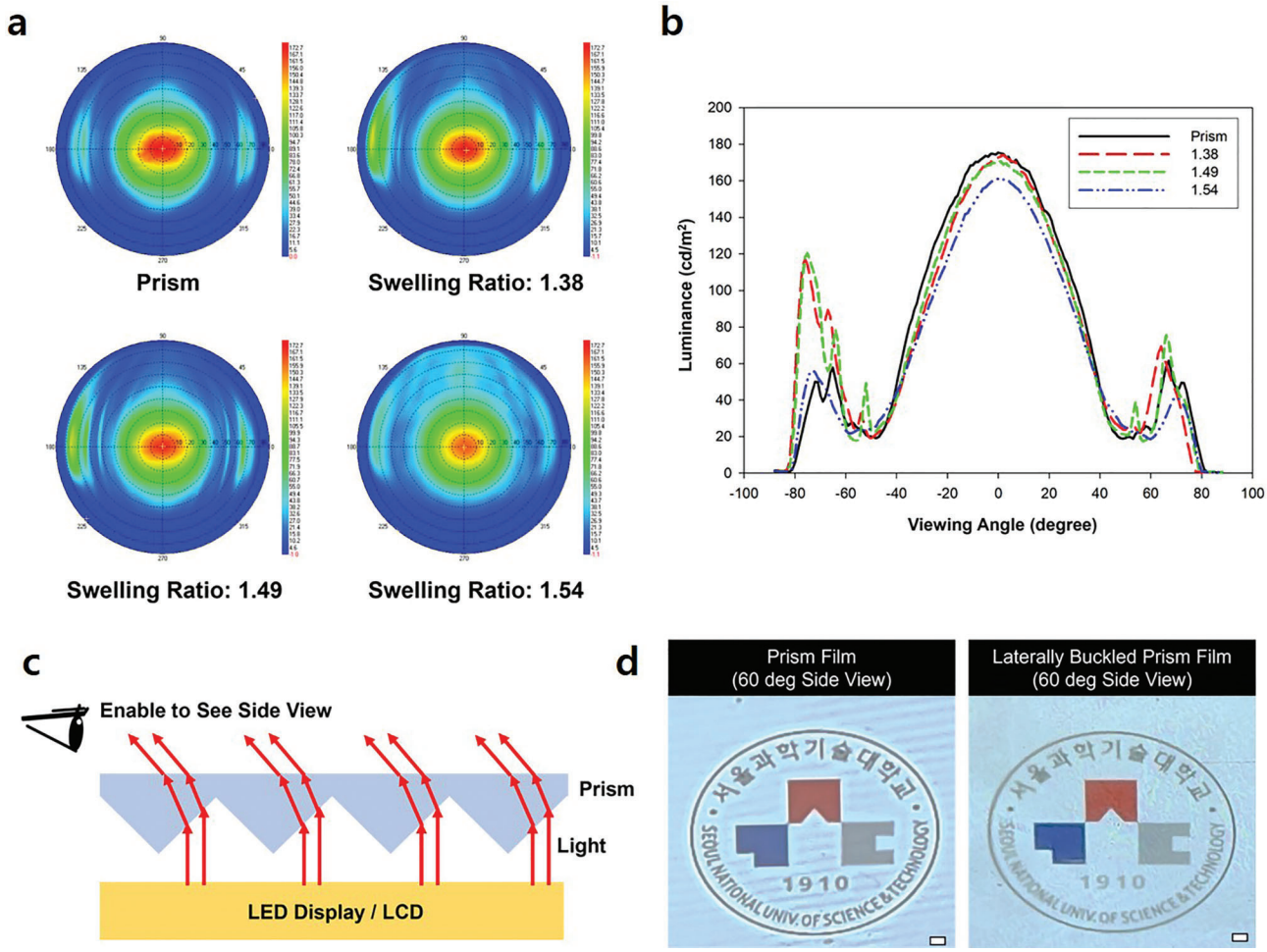

Figure 5. a) Images of the luminance for omnidirectional azimuth and viewing angles through optical films fabricated from hydrogel microprism arrays at different swelling ratios. b) Graph showing the luminance at viewing angles from −88° to 88°. c) Scheme representing the directional guidance of light through a prism array. d) Images from the side view through prism arrays with and without buckling of sharp edges. Scale bars represent 1 mm.

When the swelling ratio was 1.54, however, the collimation effect was reduced because of the scattering effect due to the strong structural deformation. Figure 5b displays a graph showing the luminance according to the viewing angle (from −88° to 88°). All prism arrays showed the highest luminance at 0°, and the maximum values were 175.3 cd m^{-2} (original prism array), 172.6 cd m^{-2} (swelling ratio = 1.38), 169.6 cd m^{-2} (swelling ratio = 1.49), and 161.2 cd m^{-2} (swelling ratio = 1.54). When integrating the luminance graph according to the viewing angle from −40° to 40°, the average luminance values of the prism arrays were 132.6 cd m^{-2} (original prism array), 124.226 cd m^{-2} (swelling ratio = 1.38), 124.8 cd m^{-2} (swelling ratio = 1.49), and 111.8 cd m^{-2} (swelling ratio = 1.54). In this work, the optimum condition to mitigate the moiré effect and maintain the optical performance is the prism array with laterally buckled edges and swelling ratio = 1.49, although there is a 5.9% luminance reduction.

Another demonstration of mitigation of the moiré effect is the directional guidance of light through a prism array. When an upside-down film with a prism array is placed on a display device, the image of the device can be refracted to the sides, which can be used to control the viewing angles of the display panels.[23,24] To compare the moiré effect of the prism arrays with and without edge buckling, we placed prism films on display panels, as shown in Figure 5c. From the side view, we can see the images in the display panels; however, moiré patterns through the straight prism arrays were observed. However, the moiré patterns were mitigated when a prism-array film with edge buckling was used (Figure 5d).

3. Conclusion

In this work, we proposed a concept to mitigate the moiré effect of prism arrays when overlapped on periodic patterns. Microprism arrays with randomly laterally buckled edges could reduce the interference of two optical films. To prepare the microprism array with laterally buckled edges, we fabricated a microprism array by hydrogel materials, which could be swollen in water. Due to the volume expansion of microprism arrays attached on a substrate, the sharp edges with applied compressive stress should be laterally deformed. While maintaining water molecules inside the hydrogel networks, we replicated the shapes with other polymers, such as PFPE and PUA. The laterally buckled prism array could

mitigate the moiré effect when we placed the optical film on conventional display devices. Additionally, we found the optimized condition that can reduce the moiré effect and maintain the optical performance. The proposed method can be used to provide optical films for more vivid display devices.

4. Experimental Section

Fabrication of the Prism Structure Master: For manufacturing a prism structure, a prism structure master with a base length of 60 µm and a height of 30 µm was made using ultrafine mold processing. After the prism structure was fabricated, a replica mold was fabricated using a transparent polymer, PDMS. PDMS has viscoelastic properties, so it does not adhere well when molding other polymers, has excellent durability, is not worn down even after patterning several times, and has excellent resistance to UV rays, so it is suitable for use as a mold when applying UV curing. After mixing the liquid PDMS prepolymer and cross-linker in a weight ratio of 10:1, the mixture was poured on the prism master and thermally cross-linked at 60 °C for 4 h or longer to prepare the prism PDMS mold.

Patterning of the Prism Structure: The prism structure made of a hydrogel was patterned on a PET film. Commercial PET films (V7610, SK microworks) coated by urethane on the films were purchased. Owing to urethane, the hydrogel polymerized by UV bonded strongly to the film.

For the hydrogel, 3 mL of HEMA, 1 g of acrylamide, and methacrylic acid were mixed according to the mass ratio as monomers, and 0.03 g of *N*,*N*′-methylenebisacrylamide was used as a crosslinker. Since the hydrogel is not a UV-curable polymer, 300 µL of a photoinitiator was added to form a UV-curable polymer. For the UV curing machine, Minuta Tech's Fusion Cure 360-08 curing machine was used, and the curing conditions were 1 min and 30 s for the primary curing and 2 h and 10 min for full curing under the condition of a wavelength of 365 nm.

Hydrogel Swelling: The fabricated prism pattern with the hydrogel was poured into water for swelling. The swelling time was 1 h, and the temperature was fixed at room temperature. The swelling ratios were measured using cubes with a volume of 0.06 cm^3, and measuring the volume after swelling. The swelling ratio of a bulk cube can differ from that of microscale prism arrays.

Patterning of the Buckled Prism Film: The swollen hydrogel was patterned again because the swollen structure returned to its original structure when the water was removed. At this time, when the swollen structure is patterned with PFPE having a fluorine group, the changed structure due to swelling is patterned as is. Therefore, an intaglio buckled prism film in which the buckling structure is located at the bottom of the prism was first made of PFPE. Figure S3 of the Supporting Information shows SEM images of the intaglio buckled prism films. Since PFPE is not a UV-curable polymer, it was formed into a UV-curable polymer by adding 5 wt% photoinitiator. For the curing conditions, primary curing was performed for 51 s, and full curing was performed for 2 h and 10 min at a wavelength of 365 nm. Then, patterning was performed once more using PUA, a UV-curable polymer, to produce a relief buckled prism film in which the buckling structure was located on top of the prism. For the curing conditions, primary curing was performed for 15 s, and full curing was performed for 2 h and 10 min at a wavelength of 365 nm.

Measurement of the Luminance: To measure the luminance of the fabricated film, the LCD viewing angle characteristic analyzer of the Regional Innovation Center-Components and Materials for Information Display was used. Eldim's EZCONTRAST XL88 was used as the luminance measurement equipment, the viewing angle was measured from −88° to 88°, and the azimuth angle was measured from 0° to 360°. The measurement time was 3 s for each sample.

Supporting Information

Supporting Information is available from the Wiley Online Library or from the author.

Acknowledgements

Y.L. and S.G.H. contributed equally to this work. This study was financially supported by Seoul National University of Science and Technology.

Conflict of Interest

The authors declare no conflict of interest.

Data Availability Statement

The data that support the findings of this study are available from the corresponding author upon reasonable request.

Keywords

buckling, deformation, hydrogels, microprism, moiré

Received: March 6, 2023
Revised: May 13, 2023
Published online: July 23, 2023

[1] B. K. Kim, J. S. Song, J. T. Kim, J. H. Jo, S. Chang, K. C. Yuk, *Appl. Opt.* **1997**, *36*, 2848.
[2] Z. Wu, Y. Zheng, *Adv. Opt. Mater.* **2018**, *6*, 1701057.
[3] Z. Wu, Y. Liu, E. H. Hill, Y. Zheng, *Nanoscale* **2018**, *10*, 18096.
[4] C. R. Dean, L. Wang, P. Maher, C. Forsythe, F. Ghahari, Y. Gao, J. Katoch, M. Ishigami, P. Moon, M. Koshino, T. Taniguchi, K. Watanabe, K. L. Shepard, J. Hone, P. Kim, *Nature* **2013**, *497*, 598.
[5] C. Jin, E. C. Regan, A. Yan, M. I. B. Utama, D. Wang, S. Zhao, Y. Qin, S. Yang, Z. Zheng, S. Shi, K. Watanabe, T. Taniguchi, S. Tongay, A. Zettl, F. Wang, *Nature* **2019**, *567*, 76.
[6] S. Liu, S. Ma, R. Shao, L. Zhang, T. Yan, Q. Ma, S. Zhang, T. J. Cui, *Sci. Adv.* **2022**, *8*, 1511.
[7] N. Li, W. Wu, S. Y. Chou, *Nano Lett.* **2006**, *6*, 2626.
[8] V. Saveljev, J. Kim, J.-Y. Son, Y. Kim, G. Heo, *Sci. Rep.* **2020**, *10*, 14414.
[9] S. Zhou, Y. Fu, X. Tang, S. Hu, W. Chen, Y. Yang, *Opt. Express* **2008**, *16*, 7869.
[10] S. M. Lubin, W. Zhou, A. J. Hryn, M. D. Huntington, T. W. Odom, *Nano Lett.* **2012**, *12*, 4948.
[11] S.-J. Byun, S. Y. Byun, J. Lee, W. M. Kim, H.-P. Kim, M. Y. Jeon, T.-S. Lee, *Opt. Express* **2014**, *22*, 3128.
[12] Z. Li, Z. Huang, Q. Yang, M. Su, X. Zhou, H. Li, L. Li, F. Li, Y. Song, *Adv. Opt. Mater.* **2017**, *5*, 1700751.
[13] D.-Y. Khang, J. A. Rogers, H. H. Lee, *Adv. Funct. Mater.* **2009**, *19*, 1526.
[14] A. Tan, L. Pellegrino, Z. Ahmad, J. T. Cabral, *Adv. Opt. Mater.* **2022**, *10*, 2200964.
[15] Z. Li, T. Zhai, Y. Wang, G. M. Wedland, X. Yin, J. Xiao, *Adv. Opt. Mater.* **2017**, *5*, 1700425.
[16] H. Qi, S. Wang, G. Huang, Y. Tu, C. Li, X. Jiang, Y. Fang, A. Wang, H. Shen, Z. Du, *Adv. Opt. Mater.* **2022**, *10*, 2102494.
[17] Z. Yan, F. Zhang, F. Liu, M. Han, D. Ou, Y. Liu, Q. Lin, X. Guo, H. Fu, Z. Xie, M. Gao, Y. Huang, J. H. Kim, Y. Qiu, K. Nan, J. Kim, P. Gutruf, H. Luo, A. Zhao, K.-C. Hwang, Y. Huang, Y. Zhang, J. A. Rogers, *Sci. Adv.* **2016**, *2*, 1601014.
[18] S. Xu, Z. Yan, K.-I. Jang, W. Huang, H. Fu, J. Kim, Z. Wei, M. Flavin, J. McCracken, R. Wang, A. Badea, Y. Liu, D. Xiao, G. Zhou, J. Lee, H. U. Chung, H. Cheng, W. Ren, A. Banks, X. Li, U. Paik, R. G. Nuzzo, Y. Huang, Y. Zhang, J. A. Rogers, *Science* **2015**, *347*, 154.

[19] H. Yoon, A. Ghosh, J. Y. Han, S. H. Sung, W. B. Lee, K. Char, *Adv. Funct. Mater.* **2012**, *22*, 3723.
[20] H. Lee, J. G. Bae, W. B. Lee, H. Yoon, *Soft Matter* **2017**, *13*, 8357.
[21] H. Lee, Y. J. Seo, J. Kim, M. J. Bae, S. Hwang, J. G. Bae, W. B. Lee, H. Yoon, *Chem. Eng. J.* **2022**, *434*, 134665.
[22] S. J. Depont Jr., R. S. Cates, P. G. Stroot, R. Toomey, *Soft Matter* **2010**, *6*, 2876.
[23] H. Yoon, S.-G. Oh, D. S. Kang, J. M. Park, S. J. Choi, K. Y. Suh, K. Char, H. H. Lee, *Nat. Commun.* **2011**, *2*, 455.
[24] H. Lee, S. G. Heo, Y. Bae, H. Lee, J. Kim, H. Yoon, *Opt Express* **2021**, *29*, 2884.
[25] D. H. Kang, S. M. Kim, B. Lee, H. Yoon, K.-Y. Suh, *Analyst* **2013**, *138*, 6230.
[26] C. Lestringant, C. Maurini, A. Lazarus, B. Audoly, *Phys. Rev. Lett.* **2017**, *118*, 165501.
[27] H.-T. Le, L.-T. Le, H.-Y. Liao, M.-J. Chem, H.-Y. Ma, H.-Y. Lee, *Crystals* **2020**, *19*, 63.